

Showcasing research into surface-enhanced photochromism from the Functional Material Chemistry Laboratory of Professor Kenta Adachi at Yamaguchi University, Japan.

**Title:** Surface-enhanced photochromic phenomena of phenylalanine adsorbed on tungsten oxide nanoparticles: a novel approach for “label-free” colorimetric sensing

We report the surface-enhanced photochromic phenomena by L-phenylalanine adsorbed on tungsten(vi) oxide ( $\text{WO}_3$ ) nanoparticles in the aqueous solution. The findings have important implications for the development of photochromic  $\text{WO}_3$  nanoparticles as highly effective colorimetric sensor probes for amino acids and related compounds.

As featured in:



See Kenta Adachi *et al.*,  
*Analyst*, 2013, **138**, 2536–2539.

RSC Publishing

[www.rsc.org/analyst](http://www.rsc.org/analyst)

Registered Charity Number 207890

# Surface-enhanced photochromic phenomena of phenylalanine adsorbed on tungsten oxide nanoparticles: a novel approach for “label-free” colorimetric sensing†

Cite this: *Analyst*, 2013, **138**, 2536

Received 9th November 2012

Accepted 22nd February 2013

DOI: 10.1039/c3an36650b

[www.rsc.org/analyst](http://www.rsc.org/analyst)

Shohei Tanaka, Kenta Adachi\* and Suzuko Yamazaki

The enhanced photochromic behaviors of the L-phenylalanine (Phe)–tungsten(vi) oxide (WO<sub>3</sub>) colloid binary aqueous solution have been investigated by means of UV-vis absorption spectrometry. The phenomena provided a potential use of the WO<sub>3</sub> nanoparticles as a colorimetric probe for sensitive “label-free” detection of Phe.

## Introduction

Amino acids are important bioactive substances, and are widely used in the food, chemical and pharmaceutical industries.<sup>1,2</sup> The deficiency of some amino acids causes various abnormalities, such as edema, lethargy, liver damage, muscle and fat loss. As a result of the increasing attention paid to human health, diagnosis and treatment of diseases, many efforts have been directed towards the accurate quantification of amino acids.<sup>3–5</sup> Currently, the most used analytical procedures to detect and characterize amino acids are based on spectroscopic, chromatographic, or electrochemical approaches. However, each approach has some drawbacks such as the need for apparatus and trained personnel, operational convenience, analysis cost, test speed, detection limit, *etc.* Recent advances in the field of amino acid sensing have focused on the use of colorimetric methods using various metal nanoparticles.<sup>6–8</sup> For instance, amino acids can be easily adsorbed on the gold or silver nanoparticle surface *via* chemical bonding and/or hydrogen bonding, which can effectively alter the behavior of the surface plasmon propagation, and this opens new avenues to quantitative amino acid assays.<sup>9,10</sup> However, many of those methods require several hours of incubation for a complete color

change,<sup>11</sup> and suffer from several inevitable shortcomings such as a low signal-to-noise ratio.<sup>12</sup>

Photochromic metal oxides (PMOs) have attracted considerable interest for many potential applications, such as information storage media, imaging devices and smart windows for controlling the temperature and light levels. Tungsten(vi) oxide (WO<sub>3</sub>) has been considered to be one of the most promising candidates for these technological applications.<sup>13–16</sup> WO<sub>3</sub> is a wide band-gap semiconductor, in which electron–hole pairs are produced upon band-gap photoirradiation. As a result, the colorless WO<sub>3</sub> material becomes blue under UV irradiation (<380 nm). Several strategies have been attempted for improving the physical, chemical stabilities, and chromogenic capability of PMOs using organic compounds.<sup>17,18</sup> More recently, we reported that the hybridization of the WO<sub>3</sub> nanoparticles into a hydrophilic organic matrix strongly enhanced their photochromism, owing to the interfacial interaction between WO<sub>3</sub> particles and the organic matrix.<sup>19</sup>

In the present study, we focus on the photochromism of the WO<sub>3</sub> colloid aqueous solution in the presence of L-phenylalanine (Phe), which has in practice been chosen among the 20 standard amino acids as a model molecule because of the hydrophilic/hydrophobic balance, and have for the first time demonstrated the potential of the WO<sub>3</sub> nanoparticles as a colorimetric probe for sensitive “label-free” detection of amino acid compounds. The unique enhanced photochromic phenomena of only the Phe molecules adsorbed on the WO<sub>3</sub> colloid surface were found.

## Results and discussion

Generally, the electrostatic interactions of amino acids with metal oxide particles are defined by the nature of their charge properties.<sup>20</sup> When the amino acids and metal oxide colloidal aqueous solution are mixed, both the amino acids and metal oxide particles experience a change in their overall charge density. For metal oxides, this change can be understood with the knowledge of their isoelectric points (*pI*) at a pH where they

Department of Environmental Science & Engineering, Graduate School of Science & Engineering, Yamaguchi University, Yamaguchi, 753-8512, Japan. E-mail: [k-adachi@yamaguchi-u.ac.jp](mailto:k-adachi@yamaguchi-u.ac.jp)

† Electronic supplementary information (ESI) available: Experimental details, figures (XRD pattern of the dried WO<sub>3</sub> colloids, UV-vis absorption spectrum of the WO<sub>3</sub> colloid solution, the adsorption isotherm of Phe onto the WO<sub>3</sub> colloid surface at various pH values, and TEM images of the WO<sub>3</sub> colloid nanoparticles), and a table (the isotherm parameters). See DOI: 10.1039/c3an36650b

carry a zero net charge. On the other hand, the overall charge of amino acids in the aqueous solution is also affected by the pH value, because of the protonation and/or deprotonation of the corresponding amine and carboxyl group. The adsorption behavior of Phe on the  $\text{WO}_3$  colloid surface was investigated by means of the HPLC technique.<sup>21</sup> The adsorption equilibrium plots of the Phe- $\text{WO}_3$  binary aqueous system are shown in Fig. 1. The pH of the binary aqueous system was in the range of 2.2–5.8. The adsorption behavior of Phe varied remarkably with the pH value; the isotherm measured at acidic pH showed a sharp initial rise, while the plots at neutral pH gradually changed. These plots were very similar to the Langmuir isotherms. Although the Langmuir isotherm has been used to resolve the molecular adsorption mechanism at surfaces, this isotherm model is not highly applicable because three equilibrated forms (cationic form [CF], zwitterionic form [ZF], and anionic form [AF]) of Phe would be present in this system. These equilibria of Phe are regulated by two acidic dissociation constants of the carboxyl ( $-\text{COOH}$ ) and amine ( $-\text{NH}_2$ ) groups ( $\text{p}K_{\text{a}1} = 2.6$  and  $\text{p}K_{\text{a}2} = 9.2$ , respectively. See Fig. S3 in the ESI†).<sup>22</sup> In order to analyze Phe's adsorption behavior onto the  $\text{WO}_3$  colloid surface, we used the following modified Langmuir isotherm equation:

$$[\text{Phe}]_{\text{ad}} = \frac{aK'_{\text{CF}}[\text{H}^+]^2[\text{Phe}]}{a(K_{\text{a}1}K_{\text{a}2} + K_{\text{a}1}[\text{H}^+] + [\text{H}^+]^2) + K'_{\text{CF}}[\text{H}^+]^2[\text{Phe}]} + \frac{aK'_{\text{ZF}}K_{\text{a}1}[\text{H}^+][\text{Phe}]}{a(K_{\text{a}1}K_{\text{a}2} + K_{\text{a}1}[\text{H}^+] + [\text{H}^+]^2) + K'_{\text{ZF}}K_{\text{a}1}[\text{H}^+][\text{Phe}]} + \frac{aK'_{\text{AF}}K_{\text{a}1}K_{\text{a}2}[\text{Phe}]}{a(K_{\text{a}1}K_{\text{a}2} + K_{\text{a}1}[\text{H}^+] + [\text{H}^+]^2) + K'_{\text{AF}}K_{\text{a}1}K_{\text{a}2}[\text{Phe}]} \quad (1)$$

where  $[\text{Phe}]_{\text{ad}}$  and  $[\text{Phe}]$  denote the concentration of Phe on the  $\text{WO}_3$  colloid surface ( $\text{mol dm}^{-2}$ ) and that in the aqueous solution ( $\text{mol dm}^{-3}$ ), respectively. Herein,  $a$  and  $[\text{H}^+]$  refer to the saturated concentration of Phe on the  $\text{WO}_3$  colloid surface ( $\text{mol dm}^{-2}$ ) and the concentration of proton in the aqueous solution ( $\text{mol dm}^{-3}$ ), respectively.  $K'_{\text{CF}}$ ,  $K'_{\text{ZF}}$ , and  $K'_{\text{AF}}$ , respectively, are the adsorption constants of CF, ZF, and AF of Phe onto the  $\text{WO}_3$  colloid surface, and are defined as follows:

$$K'_{\text{CF}} = \frac{[\text{CF}]_{\text{ad}}}{[\text{CF}]} \quad (2)$$

$$K'_{\text{ZF}} = \frac{[\text{ZF}]_{\text{ad}}}{[\text{ZF}]} \quad (3)$$

$$K'_{\text{AF}} = \frac{[\text{AF}]_{\text{ad}}}{[\text{AF}]} \quad (4)$$

where the brackets with and without the subscript 'ad' denote the concentration of each form on the  $\text{WO}_3$  colloid surface ( $\text{mol dm}^{-2}$ ) and in the aqueous solution ( $\text{mol dm}^{-3}$ ), respectively. That means, by definition,  $[\text{Phe}]_{\text{ad}} = ([\text{CF}]_{\text{ad}} + [\text{ZF}]_{\text{ad}} + [\text{AF}]_{\text{ad}})$  and  $[\text{Phe}] = ([\text{CF}] + [\text{ZF}] + [\text{AF}])$ . The adsorption parameters obtained from the least-squares curve-fitting analysis of eqn (1) under various pH conditions are summarized in Table S1 (see

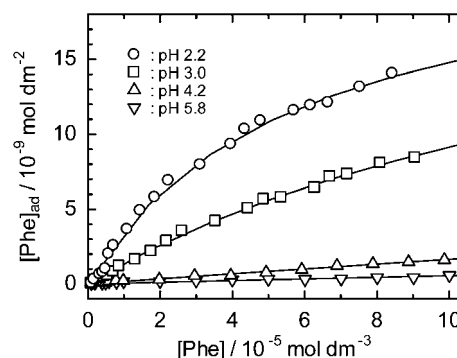


**Fig. 1** Adsorption isotherms of Phe molecules on the  $\text{WO}_3$  colloid surface at various pH values. The solid lines are the best fit of data to eqn (1) (see text). Concentration conditions:  $[\text{Phe}] = 1.0 \times 10^{-4}$  M,  $[\text{WO}_3] = 1.0 \times 10^{-6}$  to  $5.0 \times 10^{-2}$  M,  $[\text{Na}_2\text{SO}_4] = 3.3 \times 10^{-2}$  M.

ESI†). Briefly, the averaged  $K'_{\text{CF}}$  and  $K'_{\text{ZF}}$  values were calculated to be  $5.3 \times 10^{-4}$  and  $5.0 \times 10^{-6}$  dm, respectively, and the saturated concentration  $a$  was obtained to be ca.  $2.5 \times 10^{-8}$  mol  $\text{dm}^{-2}$ . Incidentally, the  $K'_{\text{AF}}$  value was unable to be obtained, because the concentration of AF was extremely smaller in the pH range of 2.2–5.8. These isotherms results clearly show that the CF and ZF of Phe are adsorbed as a monolayer on the  $\text{WO}_3$  colloid surface. Herein, note that the  $K'_{\text{CF}}$  value is about two orders larger than the value found for ZF, indicating the high affinity between the CF and the  $\text{WO}_3$  colloid surface. Since the  $\text{pI}$  value of  $\text{WO}_3$  is about 0.2–0.5,<sup>23</sup> the surface charge of the  $\text{WO}_3$  colloid is always negative under the pH conditions. We recently investigated the adsorption behavior of cationic phenothiazine (PN) dyes such as methylene blue onto the  $\text{WO}_3$  colloid surface under mildly acidic conditions (pH 4).<sup>24</sup> It was concluded that cationic PN dyes adsorbed onto the negatively charged  $\text{WO}_3$  colloid surface *via* positively charged quaternary amine groups ( $-\text{NR}_3^+$ ). Although the difference in amine groups (primary and quaternary) does exist, the result would explain that the electrostatic (attractive and/or repulsive) interactions play a central role in the adsorption of Phe onto the  $\text{WO}_3$  colloid surface. The Phe- $\text{WO}_3$  binary aqueous solutions were stable without precipitating for a week at room temperature. Indeed, TEM results showed that no agglomeration of the  $\text{WO}_3$  colloids occurred by the addition of Phe (see Fig. S4 in the ESI†).

The typical change in the absorption spectra upon UV irradiation ( $\lambda_{\text{max}} = 365$  nm) of the Phe- $\text{WO}_3$  binary aqueous solution is shown in Fig. 2. The spectra were acquired at 1 min intervals while the binary solution was continuously irradiated. As a reference, the spectral change of the as-prepared  $\text{WO}_3$  colloid aqueous solution is displayed in this figure. The spectra of the Phe- $\text{WO}_3$  binary system provide a sharp contrast in the spectral region of wavelengths longer than 500 nm. The appearance of a new absorption peak (775 nm), which is assigned to the d-d band charge transfer intervalence transition ( $\text{W}^{5+} \rightarrow \text{W}^{6+}$ ),<sup>13–15</sup> is the instrumental manifestation of the visually striking blue coloration. Interestingly, the Phe- $\text{WO}_3$  binary aqueous solution shows a stronger photochromic effect than that of the as-prepared  $\text{WO}_3$  aqueous solution by direct absorption observation (see Fig. 2(A) and (B)). The chromaticity

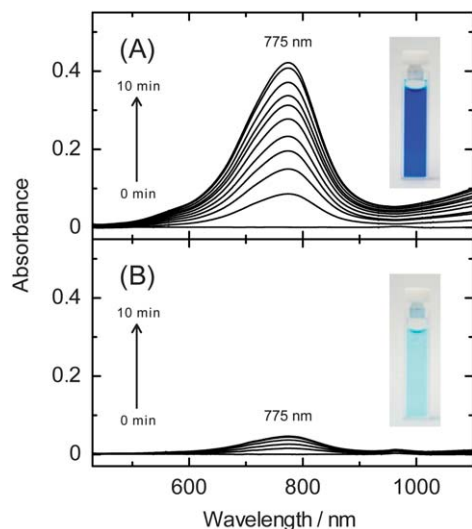


**Fig. 2** Typical absorption spectral changes of (A) the Phe- $\text{WO}_3$  binary system and (B) the as-prepared  $\text{WO}_3$  aqueous solution under UV light irradiation. Concentration conditions:  $[\text{WO}_3] = 1.0 \times 10^{-2}$  M,  $[\text{Phe}] = 1.0 \times 10^{-3}$  M,  $[\text{Na}_2\text{SO}_4] = 3.3 \times 10^{-2}$  M, pH 3.3. The insets show the photograph of the sample solutions after the irradiation for 30 min.

in the Phe- $\text{WO}_3$  binary system presents a colorless-transparent state (not shown) and a blue-transparent state (inset of Fig. 2(A)), so that the chromatism is considerably obvious to the observer's visual sensitivity. The above mentioned adsorption and photochromic results indicated that the  $\text{WO}_3$  colloid particles with the monolayer of Phe adsorbed on the surface exhibited enhanced UV photochromic responses over the as-prepared  $\text{WO}_3$  colloid particles, with the absorbance change (775 nm) being *ca.* 8 times that of the latter.

The pH dependence of the photochromism of the Phe- $\text{WO}_3$  binary aqueous system was monitored in the range of 2.2–5.8. Fig. 3 shows the time profiles of the absorbance at 775 nm of the Phe- $\text{WO}_3$  binary system and the as-prepared  $\text{WO}_3$  aqueous solution (as a reference) under UV light irradiation at the various pH values. As indicated in the figure, the initial coloration rate ( $r_0$ ) of the photochromic behaviors is given by the rate of increase of the absorbance at 775 nm ( $\text{Abs}_{775}$ ) versus time curve at  $t = 0$ .

$$r_0 = \left| \frac{d(\text{Abs}_{775})}{dt} \right|_{t=0} \quad (5)$$

The actual values were assessed by differentiating the quadratic equation fitted to the observed points. As shown in Fig. 3, although the  $r_0$  values were varied depending on the pH of the Phe- $\text{WO}_3$  binary system, there is no change of  $r_0$  values in the  $\text{WO}_3$  aqueous system. Because the adsorption isotherms of Phe onto the  $\text{WO}_3$  colloid nanoparticles are essentially dependent on pH, this difference should be ascribable to Phe forms adsorbed on the  $\text{WO}_3$  colloid surface.

From the above results of the adsorption isotherm and photochromic studies and the characterization of the as-prepared  $\text{WO}_3$  colloid particles (see ESI<sup>†</sup>), we now discuss the enhanced photochromic phenomena in the Phe- $\text{WO}_3$  binary aqueous system. The experimental results support the following facts. (i) The  $\text{WO}_3$  colloids are predominantly  $\text{WO}_3 \cdot 2\text{H}_2\text{O}$  crystal

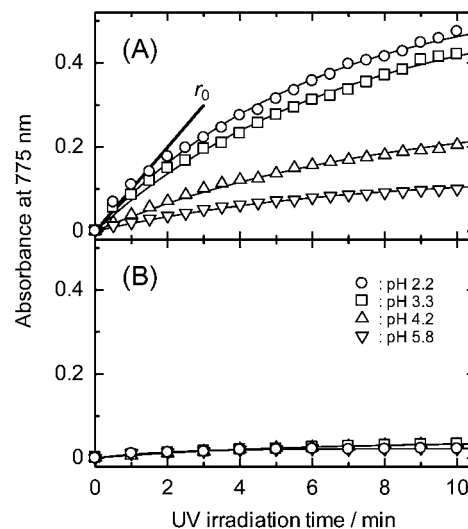
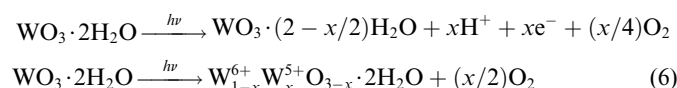


**Fig. 3** Time profiles of the absorbance at 775 nm of (A) the Phe- $\text{WO}_3$  binary system and (B) the as-prepared  $\text{WO}_3$  aqueous solution under UV light irradiation at various pH values. Concentration conditions:  $[\text{WO}_3] = 1.0 \times 10^{-2}$  M,  $[\text{Phe}] = 1.0 \times 10^{-3}$  M,  $[\text{Na}_2\text{SO}_4] = 3.3 \times 10^{-2}$  M.

particles (XRD, see Fig. S1 in the ESI<sup>†</sup>); (ii) the electrostatic interaction between the Phe molecules (especially cationic amine groups ( $-\text{NH}_3^+$ )) and the negatively charged  $\text{WO}_3$  colloid surface contributes to the adsorption behavior of Phe onto the  $\text{WO}_3$  colloid surface (adsorption isotherm); (iii) the pH value has a great impact on both the adsorption and photochromic behaviors in the Phe- $\text{WO}_3$  binary aqueous system (adsorption isotherm and UV-vis absorption). Up to now, a number of studies have been carried out on the photochromism performance, and a model of double insertion/extraction of ions and electrons was developed to elucidate the photochromic mechanism of  $\text{WO}_3$ . The corresponding photochromic reaction process can be described by the following equation.<sup>25</sup>



When crystalline  $\text{WO}_3 \cdot 2\text{H}_2\text{O}$  is irradiated by UV light, electrons are excited to the conduction band, leaving holes in the valence band. The photogenerated holes can weaken the O-H bonds of water molecules in the  $\text{WO}_3 \cdot 2\text{H}_2\text{O}$  and cause the water molecules to decompose into protons and highly reactive oxygen radicals. The oxygen radicals may bind to each other and be released to the atmosphere in the molecular form. Then, the separated protons ( $\text{H}^+$ ) will combine with  $\text{O}^{2-}$  in the chromogenics to form  $\text{H}_2\text{O}$  with the help of proton energy. Therefore, the photogenerated electron-hole pairs give rise to the reduction of transparent  $\text{W}^{6+}$  ions into colored  $\text{W}^{5+}$  ions. Given that the displacement of hydrogen from the organic component toward the  $[\text{WO}_6]$  framework enhances the photochromism under the excitation described above, it is reasonable to assume that Phe adsorbed onto the  $\text{WO}_3$  colloid surface *via* the  $-\text{NH}_3^+$  group acts as the proton source and  $\text{W}^{6+}$  ions in  $\text{WO}_3 \cdot 2\text{H}_2\text{O}$  nanocrystal are preferentially photoreduced. Indeed, many researchers have



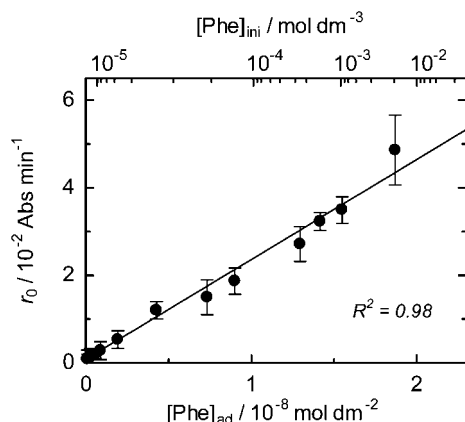


**Fig. 4** Dependence of the initial coloration rate ( $r_0$ ) on the concentration of Phe adsorbed on the  $\text{WO}_3$  colloid surface ( $[\text{Phe}]_{\text{ad}}$ ; lower axis) and the initial concentration of Phe ( $[\text{Phe}]_{\text{ini}}$ ; upper axis). The straight line indicates the best fitting curves obtained by the least-squares method. The magnitude of the error bars was calculated from the uncertainty given by five independent measurements.

concluded that  $\text{WO}_3$  photochromism enhancing compounds such as polyethyleneimine,<sup>26</sup> alkylammonium,<sup>27</sup> etc., have cationic amine groups as a common chemical structure.

The analytical performance of the enhanced photochromism phenomenon was investigated by measuring various Phe concentrations in the  $\text{WO}_3$  colloid aqueous solution. For the rapid monitoring of Phe concentration in a sample solution, the use of the initial coloration rate ( $r_0$ ) is suitable, and would gain wide acceptance. As shown in Fig. 4, a linear relationship between the  $r_0$  value and the concentration of Phe on the  $\text{WO}_3$  colloid surface ( $[\text{Phe}]_{\text{ad}}$ ), which was calculated using the adsorption parameters obtained in this study, was obtained in the range of ca.  $1.0 \times 10^{-10}$  to  $1.9 \times 10^{-8}$  mol dm<sup>-2</sup> (corresponding to the range of  $7.8 \times 10^{-6}$  to  $5.1 \times 10^{-3}$  M at pH 2). The correlation coefficient  $R^2$  was 0.98 (this value includes the batch-to-batch variation in the  $\text{WO}_3$  colloid solution processing). It is clearly indicated that the enhanced photochromic phenomenon in the Phe- $\text{WO}_3$  binary aqueous system is reflected in the very small amount of Phe adsorbed on the  $\text{WO}_3$  colloid surface. Under optimal conditions, a detection limit of  $9.0 \times 10^{-12}$  mol dm<sup>-2</sup> ( $1.0 \times 10^{-6}$  M at pH 2) for Phe was estimated from 3SD (SD was the standard deviation of 5 measurements of a blank solution).

In summary, we have demonstrated, for the first time, the use of surface-enhanced photochromic phenomena for sensitive label-free Phe sensing using the  $\text{WO}_3$  colloid nanoparticles as a colorimetric probe. A good linear correlation between the initial coloration rate and the surface concentration of Phe on the  $\text{WO}_3$  can be obtained over 3 orders of magnitude, and a low detection limit for Phe of  $9.0 \times 10^{-12}$  mol dm<sup>-2</sup> ( $1.0 \times 10^{-6}$  M at pH 2) can be achieved. A more detailed study of the surface-enhanced photochromism of the  $\text{WO}_3$  colloid aqueous system is currently under investigation using other amino acids and related compounds, and will be reported elsewhere.

## Acknowledgements

This study was partially supported by the Scientific Research of the Grant-in-Aid for Young Scientists (B) (no. 24750069) from

MEXT Japan. TEM and XRD measurements documented in this report were performed at the Innovation Center and the Center for Instrumental Analysis, Yamaguchi University, respectively.

## Notes and references

- 1 K. Imura and A. Okada, *Nutrition*, 1998, **14**, 143–148.
- 2 P. Felig, *Annu. Rev. Biochem.*, 1975, **44**, 933–955.
- 3 E. W. Yemm, E. C. Cocking and R. E. Ricketts, *Analyst*, 1955, **80**, 209–214.
- 4 M. Roth, *Anal. Chem.*, 1971, **43**, 880–882.
- 5 M. Dauner and U. Sauer, *Biotechnol. Prog.*, 2000, **16**, 642–649.
- 6 O. Lioubashevski, V. I. Chegel, F. Patolsky, E. Katz and I. Willner, *J. Am. Chem. Soc.*, 2004, **126**, 7133–7143.
- 7 J. M. Wessels, H. G. Nothofer, W. E. Ford, F. V. Wrochem, F. Scholz, T. Vossmeier, A. Schroedter, H. Weller and A. Yasuda, *J. Am. Chem. Soc.*, 2004, **126**, 3349–3356.
- 8 J. Gao, J. Fu, C. Lin, J. Lin, Y. Han, X. Yu and C. Pan, *Langmuir*, 2004, **20**, 9775–9779.
- 9 D. R. Bae, W. S. Han, J. M. Lim, S. Kang, J. Y. Lee, D. Kang and J. H. Jung, *Langmuir*, 2010, **26**, 2181–2185.
- 10 L. Li and B. Li, *Analyst*, 2009, **134**, 1361–1365.
- 11 S. Yamazaki, T. Yamate and K. Adachi, *Colloids Surf., A*, 2011, **392**, 163–170.
- 12 S. Lee and V. H. Pérez-Luna, *Anal. Chem.*, 2005, **77**, 7204–7211.
- 13 B. Abécassis, F. Testard and T. Zemb, *Soft Matter*, 2009, **5**, 974–978.
- 14 K. V. Yumashev, A. M. Malyarevich, N. N. Posnov, I. A. Denisov, V. P. Mikhailov, M. V. Artemyev and D. V. Sviridov, *Chem. Phys. Lett.*, 1998, **288**, 567–575.
- 15 T. He and J. Yao, *Prog. Mater. Sci.*, 2006, **51**, 810–879.
- 16 T. He and J. Yao, *J. Mater. Chem.*, 2007, **17**, 4547–4557.
- 17 K. Kuboyama, K. Hara and K. Matsushige, *Jpn. J. Appl. Phys.*, 1994, **33**, 4135–4136.
- 18 W. Qi, H. Li and L. Wu, *J. Phys. Chem. B*, 2008, **112**, 8257–8263.
- 19 K. Adachi, T. Mita, S. Tanaka, K. Honda, S. Yamazaki, M. Nakayama, T. Goto and H. Watarai, *RSC Adv.*, 2012, **2**, 2128–2136.
- 20 A. Vallee, V. Humblot and C.-M. Pradier, *Acc. Chem. Res.*, 2010, **43**, 1297–1306.
- 21 K. Adachi, S. Tanaka, S. Yamazaki, H. Takechi, S. Tsukahara and H. Watarai, *New J. Chem.*, 2012, **36**, 2167–2170.
- 22 R. M. C. Dawson, D. C. Elliott, W. H. Elliott, K. M. Jones, *Data for Biochemical Research*, Oxford University Press, USA, 1989.
- 23 M. Kosmulski, *Chemical Properties of Material Surfaces*, Marcel Dekker Inc., New York, USA, 2001.
- 24 K. Adachi, T. Mita, T. Yamate, S. Yamazaki, H. Takechi and H. Watarai, *Langmuir*, 2010, **26**, 117–125.
- 25 J. G. Zhang, D. K. Benson, C. E. Tracy, S. K. Deb, A. W. Czanderna and C. Bechinger, *J. Electrochem. Soc.*, 1997, **144**, 2022–2026.
- 26 Y. Nagaoka, S. Shiratori and Y. Einaga, *Chem. Mater.*, 2008, **20**, 4004–4010.
- 27 S. Liu, L. Xu, F. Li, B. Xu and Z. Sun, *J. Mater. Chem.*, 2011, **21**, 1946–1952.